Energy Engineering

Tech Science Press

DOI: 10.32604/ee.2022.018185

ARTICLE

Classification of Transmission Line Ground Short Circuit Fault Based on Convolutional Neural Network

Tao Guo, Gang Tian, Zhimin Ao*, Xi Fang, Lili Wei and Fei Li

Tongren Power Supply Bureau of Guizhou Power Grid Co., Ltd., Tongren, 554300, China

*Corresponding Author: Zhimin Ao. Email: Aozhimin1983@163.com

Received: 06 July 2021 Accepted: 15 September 2021

ABSTRACT

Ground short circuit faults in current transmission lines are common in the power systems. In order to prevent the power system from aggravating the accident caused by short-circuit faults of transmission lines, a novel convolutional neural network (CNN) model is constructed to identify the short-circuit fault of the transmission line in the power system. The CNN model is mainly consisted of five convolutional layers, three max-pooling layers, one concatenate layer, one dropout layer, one fully connected layer, and a Softmax classifier. This method uses a fixed time window to intercept system short-circuit fault data, extracts the deep features of these data from the training samples, and then corresponds the extracted features to labels one-to-one. Finally, in PSCAD/EMTDC, the new England 10 machine 39 nodes are taken as an example to realize the simulation. The experimental results show that the CNN model can quickly and accurately identify the short-circuit fault types, and the optimal model accuracy rate reaches 99.95%. The results of this manuscript -have positive effect on enhancing the disaster prevention capability and the operation stability of transmission lines.

KEYWORDS

Convolutional neural networks; transmission line; fault; classification

1 Introduction

Transmission lines are considered as an important part of the power system, connecting power plants and end users. With the continuous development of society and economy, the power demand response is increasing, and the power grid is rapidly developing [1,2]. It has become a smart grid with wide coverage, high voltage level, large load capacity, and complex line conditions. The natural environment in which transmission lines are located is mostly harsh, and they are often affected by weather, external environment and other factors, which could easily cause short circuit failures of transmission lines. Therefore, it is of great significance to ensure the safe and efficient operation of transmission lines [3–5].

In the process of a transmission line failure, transient signals such as voltage, current, and frequency contain a large amount of fault information [6–9]. In this regard, comprehensive analysis of short-circuit faults and accurate diagnosis of faults are crucial to ensure the stable and safe operation of transmission lines.

This work is licensed under a Creative Commons Attribution 4.0 International License, which permits unrestricted use, distribution, and reproduction in any medium, provided the original work is properly cited.

In the development and application of transmission line fault diagnosis, many researchers have constantly explored new and accurate fault classification algorithms and models for decades [10–12]. For instance, Jiang et al. [13] presented a new adaptive fault protection scheme for transmission lines, in which Clarke transformation (CT) was used to produce fault detection indexes. But the versatility and scalability of these indicators need to be further verified. Mahanty et al. [14] constructed a model for fault classification in transmission lines based on radial basis function network (RBFN). Mirzaei et al. [15] compared the faults classification results of FNN, RBFN and PNN in an IEEE 13-node test feeder. And the results proved that PNN performed better than the other two. Furthermore, Parikh et al. [16] used support vector machine (SVM) to classify fault of transmission line, and the results indicated that the proposed method was effective. Recently, Fahim et al. [17] presented a self-attention convolutional neural network (SAT-CNN) for transmission line faults classification and final results demonstrated that this model made precise classification of transmission line faults with high accuracy. Although the aforementioned fault classification models have proved to be valid and advantageous, these methods are limited by large dependence on data features, slow model training speed, and weak generalizability.

After analysing and demonstrating the problem of fault classification in transmission lines in detail, we aim to construct a novel model to classify the short-circuit fault by referring to models with good performance used in the previous literatures [18,19]. The short-circuit fault data contain a lot of information, so it is necessary to find the key features. And CNN has the ability to extract deep features from complex data, so CNN is a feasible and effective tool. The problem of short-circuit fault detection in this paper is decomposed into two steps: firstly, a fixed time window is used to extract the data near the starting time of the fault, then these data are employed to classify faults based on the CNN model.

2 Materials and Data

In the initial period after the power system failed, the voltage, current and other electrical quantities near the fault point would change drastically. CNN could capture the changes between node data, which has significant advantages in processing high-dimensional, non-linear feature classification problems.

The experimental data are generated automatically in batches after setting the component parameters and related configurations of time domain simulation, which solves the problem of obtaining experimental data. Next, these simulated data are applied to verify the effectiveness and accuracy of using CNN to solve ground short circuit fault classification problems.

2.1 Experimental Data Generation

In PSCAD/EMTDC, the New England 10 machine 39 node is employed to realize the joint simulation using the Python API interface. The experimental code runs on a 2.3 GHz Haswell MacBook Pro, Ubuntu Linux 14.04. the total running time of the system is shortened to 0.25 s, and the step lengths of the simulation system iteration and the simulation output are set to 10 μs and 0.2 ms, respectively. The starting point of the fault is set at the time when the system runs stably for 50 ms, and the fault will be removed when the fault runs for 100 ms. All the data fragments used in the experiment have a duration of less than 100 ms in order to identify the fault before the fault was cleared by itself.

The loads in the simulation are randomly selected, and the distribution of the number of load units conforms to the normal distribution. Meanwhile, a random non-linear coefficient is added to the selected load intended to increase or decrease a certain proportional load on the basis of the steady-state load, in which the load coefficient is ranged between 0.4 to 1.5. Ten types of short-circuit faults are selected in this manuscript and the fault points are uniformly set on the transmission line near the bus to simplify the model of the system. 24 possible failure points are preset in the system and only one failure point is triggered at a time to cause a short-circuit fault. The data acquisition channels are the transmitted active power and reactive power, the voltage per-unit value and the phase angle of the A-phase voltage in 32 important transmission lines. As shown in Fig. 1, the blue points are the locations of the 24 fault points and the red numbers represent the locations of the 32 selected transmission lines.

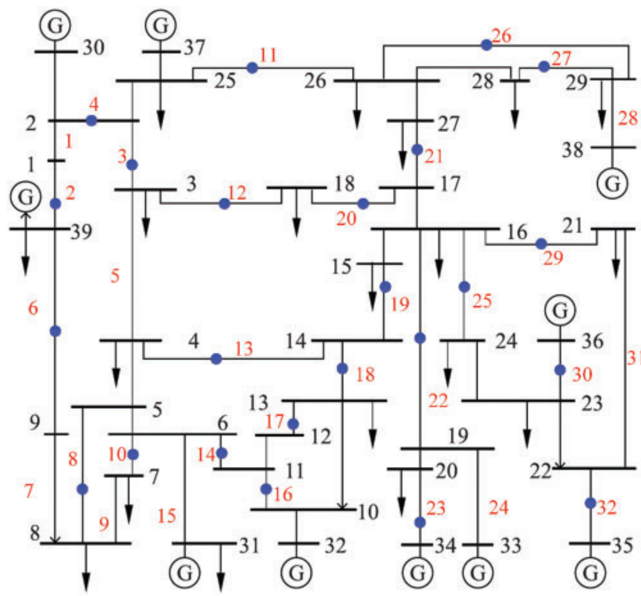

Figure 1: Electrical connection diagram of the New England 10 machines and 39 node system

The system is designed to simulate ground short circuit faults that occur in real power systems under different operating conditions and it takes into account the fault transition resistance at the same time. A total of 5000 original data samples are generated in the simulation. By recording the actual load operation of each simulation, the number of actual adjustments parameters of each load is counted. The 5000 statistical samples are divided into seven groups and the result is plotted in Fig. 2. The x-axis is the load number, the y-axis represents the batch and the z-axis is the adjustments times of the load in the current batch. As a result, the load distribution of each simulation has no obvious regularity, which increases the diversity of the data.

Fig. 3 shows the change of electrical quantity on the line between the 7th and 8th busbars when a phase A ground fault arisen on the line between the 39th and 9th busbars.

As shown in Fig. 3, the four electrical quantities on a single line have significant fluctuation characteristics by comparing whether the fault occurs. Therefore, it is necessary to select an appropriate fault data length and then slice the original data to obtain the fault feature matrix. This method selects 40 ms simulation data as the feature matrix after the fault takes place and extracts a set of data every 0.2 ms, so the total length of the data slice is 200. Each group of data is composed of four electrical quantities of 32 transmission lines. Eventually, a feature matrix of $5000 \times 200 \times 128$ is formed. There are 10 preset short-circuit fault types, including single-phase-to-ground short-circuit, two-phase-to-ground short-circuit, two-phase-to-phase short-circuit, and three-phase short-circuit. The fault types are sequentially coded as 1, 2, 3, . . . , 10, and the coding results are listed in Table 1.

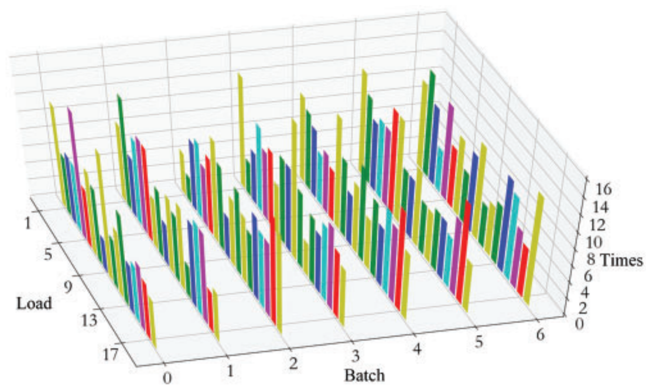

Figure 2: Load distribution after processing

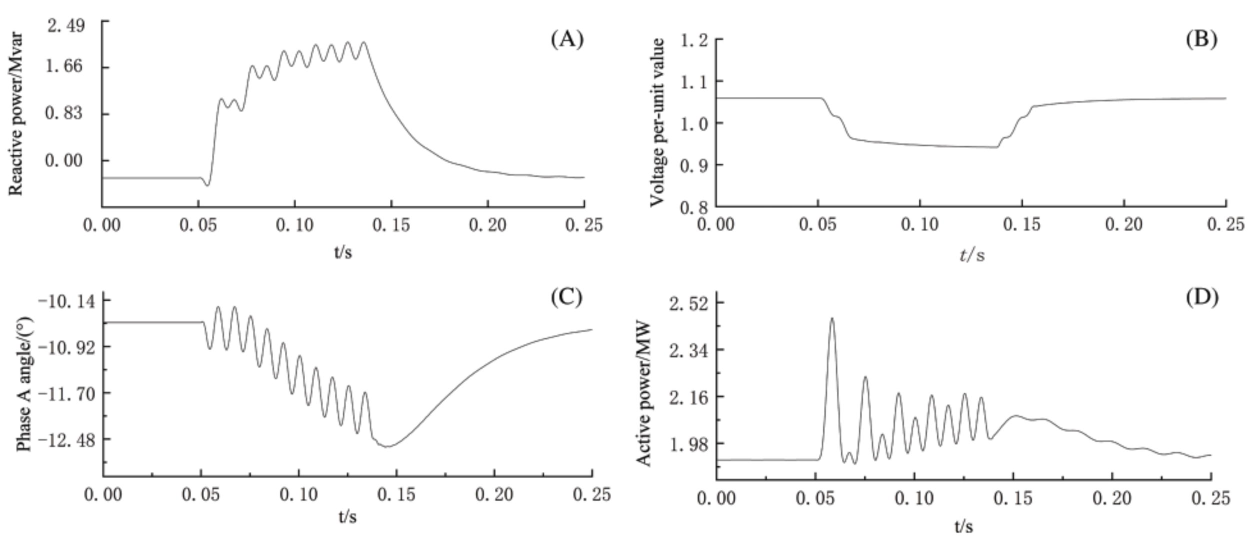

Figure 3: Waveforms of related electrical quantities near the short-circuit point

Table 1: Coding process of ground short circuit fault type

Fault type	Labels
Phase A fault grounding	1
Phase B fault grounding	2
Phase C fault grounding	3
AB phase failure	4
AC phase failure	5
BC phase failure	6
ABC phase failure	7

(Continued)

Table 1 (continued)

Fault type	Labels
Fault grounding of phase AB	8
Fault grounding of phase AC	9
Fault grounding of phase BC	10

2.2 Experimental Data Preprocessing

Fault data include power grid information of different dimensions and different indicators. The original data cannot extract key features uniformly and effectively, so various types of electrical data need to be preprocessed. The Z-score standardization method is often applied for samples with multiple classification algorithms and large numerical distributions. This method has strong adaptability, which could effectively improve data distribution characteristics and accelerate model convergence. Z-score standardization is employed to preprocess fault data with taking into account its characteristics, and its calculation formula could express as follows:

$$x' = \frac{x - \mu}{\sigma} \tag{1}$$

where x and x' represent the original value and the normalized value, respectively. μ is the average of each column and σ is the standard deviation of each column. The data structure remains the same after normalization.

After the sample preprocessing is completed, the data set needs to be divided into the training and the test sets. The Sample set partitioning based on joint X-Y distances (SPXY) method is adopted to divide the dataset [20] and the sample are eventually divided into the training set and test set according to the ratio of 8:2.

3 Methods

3.1 Convolutional Neural Network Structure

Convolutional neural networks have been widely applied in target recognition [21–23] and classification [24–26]. The constructed CNN architecture and its parameter settings have been listed in Fig. 4. Additionally, the ReLU excitation function is connected after each convolution layer, which has higher computational efficiency and better convergence effect than functions such as sigmoid and tanh. The epoch and batch size are set to 30 and 32, respectively. In this scenario, the process of CNN training could be briefly summarized as the following steps. First, the 200×128 input matrix is resized to a 128×128 square matrix. Second, the matrix is convolved by three convolutional layers, which have the same 64 filters with the size of 3×3, 5×5, 7×7, respectively. And then, the outputs are fused by the concatenate layer. Third, the feature matrix with dimensions of $128 \times 128 \times 192$ is down sampled by the Max pooling layer with the size of 2×2. Fourth, the feature matrix continues to be successively convolved and downsampled until its dimension is $15 \times 15 \times 256$. Fifth, the feature matrix with dimension of $15 \times 15 \times 256$ is input to fully connected layer to convert the data into a vector. And the dropout layer is adopted to raise generalization capability. Finally, the probability results of various faults are output through the Softmax classifier.

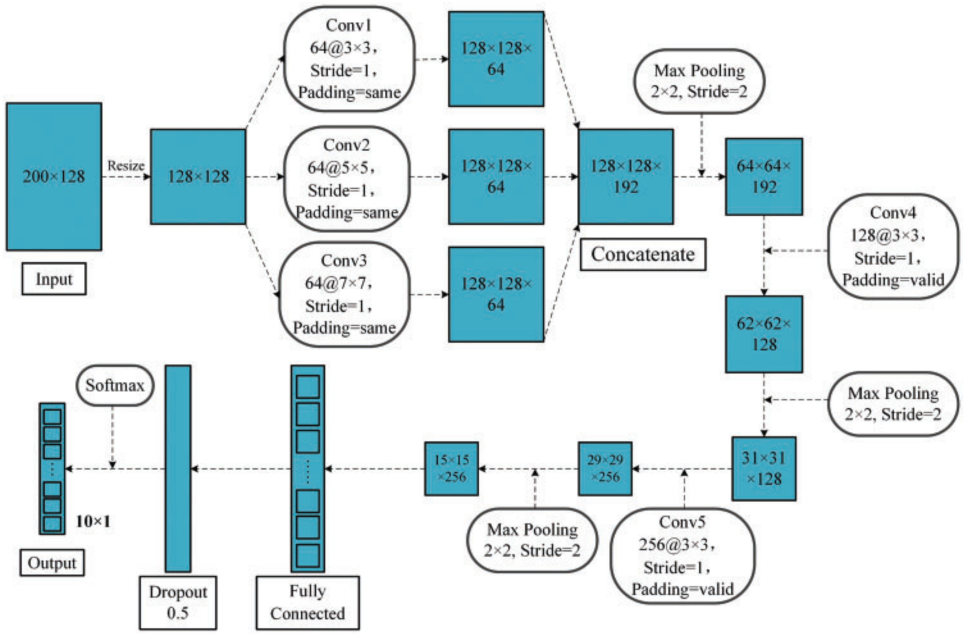

Figure 4: CNN classifier architecture

3.2 Assessment Parameters

Accuracy and Mean Absolute Error (MAE) are used as two evaluation quality indicators to assess the reliability of the CNN model. The Accuracy and MAE are defined as follows:

$$Accuracy = \frac{N_r}{N} \tag{2}$$

$$MAE = \frac{1}{n}\sum_{i=1}^{n} |L_i - L_i'| \tag{3}$$

where N_r is the number truly classified as correct and N is the total number. n is the data length of the test set, L and L' represent the initial label value of model and the converted value of the model output, respectively.

4 Results and Discussion

Fig. 5 displays the changes in both model's accuracy and MAE as the epoch increases. As it shows, the CNN model's MAE is highly correlated with accuracy. In the initial stage, the accuracy of the model output is significantly improved with the rapid decrease of the MAE. As the number of iterations increased, the changes in MAE and accuracy gradually become smoother. In order to avoid the model falling into local oscillations, the learning rate is adjusted adaptively to the training speed so that the model tends to converge. When the effect no longer improves, the model can promote convergence by reducing the value of the current learning rate. When the iteration ends, the CNN model has completely converged, indicating that the model performs well. As plotted in Fig. 6, the learning rate varies with the training number.

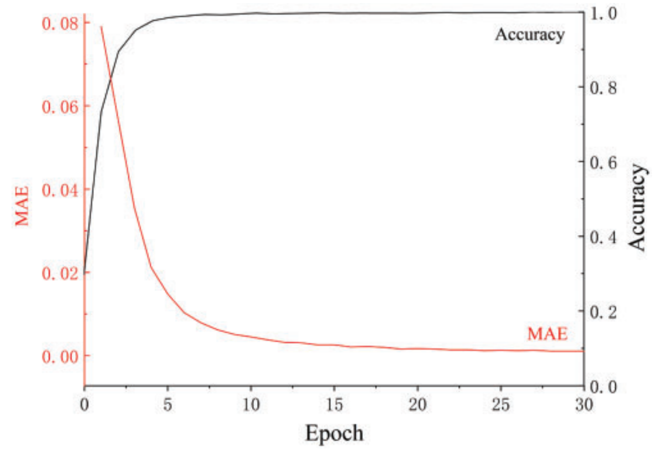

Figure 5: Curve chart of accuracy and loss value for the fault classification

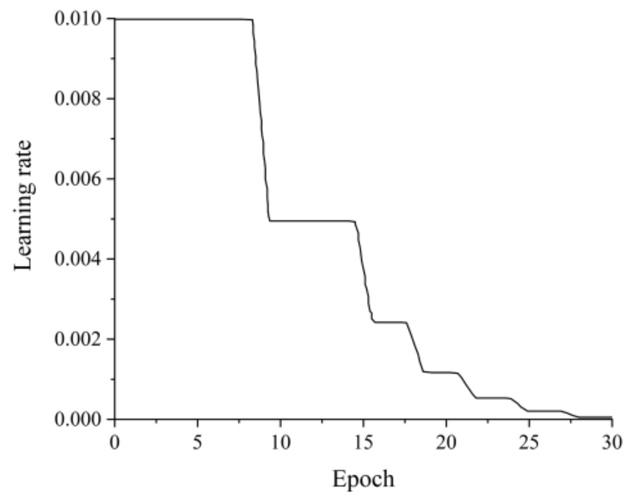

Figure 6: Adaptive learning rate change ladder diagram

Due to the inexplicability of using deep learning algorithm, the final result is obtained by averaging multiple evaluations. The results reveal that the constructed CNN model could quickly and accurately complete the detection of the line fault in the case of different types of short-circuit faults on the line, and the accuracy of the fault classification reaches 99.95%. This method uses offline training and online detection, which significantly reduce the pressure of the system to perform repetitive calculations online.

4.1 Comparison of Different Data Lengths

To meet good sensitivity, the power system should quickly identify and remove the fault after the fault occurs. The CNN model in this manuscript requires the system to collect enough failure data, but the data length should be appropriate. On the one hand, if the model collects too many samples, the duration of the failure will be prolonged and thus the system will be at the risk of cascading failures. On the other hand, high-voltage circuit breakers have inherent operating time, and acquisition time would affect the system's requirements for the protection quick action. Therefore, this section analyzes the influence of different sample data lengths on the model's output results. The performance of the CNN model under different input data lengths is shown in Table 2.

Table 2: Performance of the CNN model under different input data length

Data length	Accuracy	MAE	Iteration number
20 ms	99.12%	2.84×10^{-4}	38
30 ms	99.38%	1.98×10^{-4}	36
40 ms	99.95%	1.94×10^{-4}	30
50 ms	99.84%	2.47×10^{-4}	44

As can be seen from Table 2, the accuracy of the model does not change obviously with the data length increasing, which reflects that the data length has a small effect on the accuracy. But when the data length is 40 ms, the model has a slight advantage of smaller MAE and less convergence, which indicates that the intercepted data are able to present sufficient characteristics during this period. Therefore, selecting an appropriate data length is helpful to ensure the response speed and stability of the model.

4.2 Comparison of Different Learning Rates

The learning rate is an essential factor that determines the quality of the model's output during the application of convolutional neural network. It also plays a key role when using the loss function to adjust the network variables. For example, if the learning rate is too large, the model would not converge and the global optimum point cannot be found. On the contrary, if the learning rate is too small, the training number would increase, which would affect the overall efficiency of the system. So, this section compares the model results in the case of a fixed learning rate of 0.01 and an adaptive learning rate. The relationship between the MAE and the number of training in the two cases are demonstrated in Fig. 7.

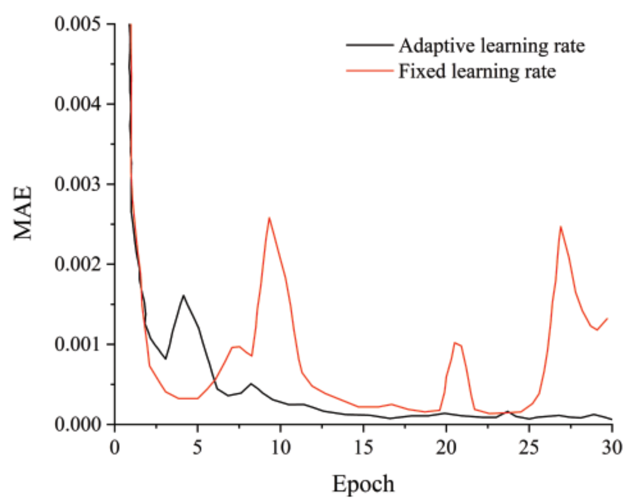

Figure 7: Comparison of different learning rates based on the CNN model

Fig. 7 indicates that the adaptive learning rate could improve the model's fit in the later stage of training, which is better than the fixed learning rate. In general, the adaptive learning rate can effectively improve the performance of the model.

4.3 Comparison of Different Data Volumes

In fact, the distribution status of the power generation side and the power consumption side change dynamically during the operation of the power system, which means that the model need to consider the adaptability of the initial accumulated fault sample data to the power system topology.

Therefore, this section compares the model performance under different data volumes and the results are provided in Fig. 8. As can be seen from Fig. 8, different sample sizes are of direct impact on the stability and accuracy of the model. Under the same conditions, as the sample data increases, the more accurate the model's output results are and the faster it converges. However, the amount of data should not be too rich because there may be deviations in the long-term samples. Furthermore, large samples would enhance the difficulty of network model training and raise the computational cost.

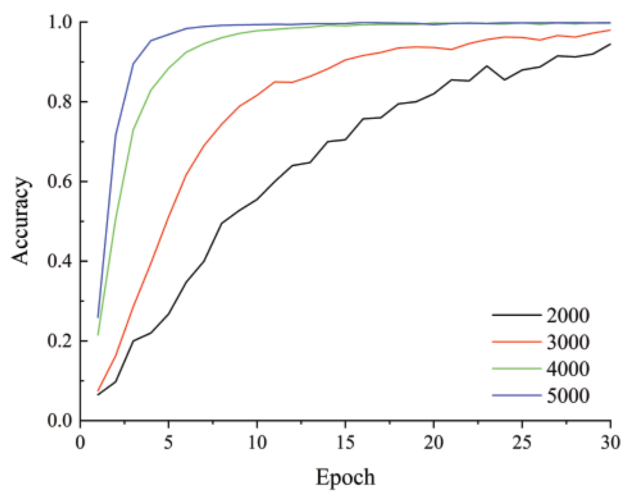

Figure 8: Impact of different data sample sizes on the model

4.4 Comparison of Different Algorithms

Fault classification of transmission line not only greatly depends on the machine learning algorithm used, but the selection of hyperparameters in different methods also have a certain impact on the classification results. Conventional machine learning algorithms include BP neural network, convolutional neural network, long and short-term memory network (LSTM) and so on. This section aims to compare the performance of four common algorithms in identifying fault types and the results are concluded in Table 3.

It could be clearly seen from Table 3 that the CNN model has obvious competitive advantages with the lowest error and the highest accuracy, which is superior to the other three machine learning algorithms. This proves that the CNN model can accurately and quickly identify the types of short-circuit faults of transmission lines.

Table 3: Performance comparison of different algorithms

Method	Accuracy	MAE	Iteration number	Iteration time (s)
BP	96.87%	1.62×10^{-3}	25	214
GRNN	95.28%	2.15×10^{-3}	42	587
LSTM	98.36%	1.34×10^{-3}	35	485
CNN	99.95%	1.94×10^{-4}	30	356

This section analyzes the influence of data length and data volume on the model's output, which clarifies the advantages of using adaptive learning rate and CNN model. This method could complete the response to the fault within 100 ms after the fault occurred and correctly identify the types of short-circuit faults of transmission lines. In the future, this method can be further integrated into the stability control system, which can reduce the damage to the power system caused by the short-circuit fault.

5 Conclusions

In this manuscript, convolutional neural networks are implemented in fault diagnosis of transmission lines, and a fault classification model based on the CNN model is proposed, which could classify and identify short-circuit faults of power system transmission lines with satisfactory results. This method has both high scalability, adaptability, good application prospects. However, the limitation of fault classification in this manuscript is that it only works for short-circuit faults of transmission lines. The establishment of a more comprehensive fault classification model would be the next improvement direction.

Funding Statement: The authors received no specific funding for this study.

Conflicts of Interest: The authors declare that they have no conflicts of interest to report regarding the present study.

References

1. Chen, K. J., Hu, J., He, J. L. (2018). Detection and classification of transmission line faults based on unsupervised feature learning and convolutional sparse autoencoder. *IEEE Transactions on Smart Grid, 9(3),* 1748–1758. DOI 10.1109/tsg.2016.2598881.
2. Tong, H., Qiu, R. C., Zhang, D., Yang, H., Ding, Q. et al. (2021). Detection and classification of transmission line transient faults based on graph convolutional neural network. *Csee Journal of Power and Energy Systems, 7(3),* 456–471. DOI 10.17775/cseejpes.2020.04970.
3. Jamehbozorg, A., Shahrtash, S. M. (2010). A Decision-tree-based method for fault classification in single-circuit transmission lines. *IEEE Transactions on Power Delivery, 25(4),* 2190–2196. DOI 10.1109/tpwrd.2010.2053222.
4. Mahamedi, B., Zhu, J. G. (2013). Fault classification and faulted phase selection based on the symmetrical components of reactive power for single-circuit transmission lines. *IEEE Transactions on Power Delivery, 28(4),* 2326–2332. DOI 10.1109/tpwrd.2013.2265711.
5. Adu, T. (2002). An accurate fault classification technique for power system monitoring devices. *IEEE Transactions on Power Delivery, 17(3),* 684–690. DOI 10.1109/tpwrd.2002.1022787.

6. Valente, W. A. G., Honorio, L. D., de Oliveira, E. J., Barbosa, D. D., Boas, E. R. V. (2016). A successive geometric segmentation approach applied to double-circuit transmission lines fault classification and location. *Journal of Control Automation and Electrical Systems, 27(4),* 452–462. DOI 10.1007/s40313-016-0252-4.
7. Dasgupta, A., Nath, S., Das, A. (2012). Transmission line fault classification and location using wavelet entropy and neural network. *Electric Power Components and Systems, 40(15),* 1676–1689. DOI 10.1080/15325008.2012.716495.
8. Chen, Y. Q., Fink, O., Sansavini, G. (2018). Combined fault location and classification for power transmission lines fault diagnosis with integrated feature extraction. *IEEE Transactions on Industrial Electronics, 65(1),* 561–569. DOI 10.1109/tie.2017.2721922.
9. Gomes, A. D., Costa, M. A., de Faria, T. G. A., Caminhas, W. M. (2013). Detection and classification of faults in power transmission lines using functional analysis and computational intelligence. *IEEE Transactions on Power Delivery, 28(3),* 1402–1413. DOI 10.1109/tpwrd.2013.2251752.
10. Saber, A., Emam, A., Amer, R. (2016). Discrete wavelet transform and support vector machine-based parallel transmission line faults classification. *IEEJ Transactions on Electrical and Electronic Engineering, 11(1),* 43–48. DOI 10.1002/tee.22187.
11. Belagoune, S., Bali, N., Bakdi, A., Baadji, B., Atif, K. (2021). Deep learning through LSTM classification and regression for transmission line fault detection, diagnosis and location in large-scale multi-machine power systems. *Measurement, 177,* 14. DOI 10.1016/j.measurement.2021.109330.
12. Dash, P. K., Samantaray, S. R., Panda, G. (2007). Fault classification and section identification of an advanced series-compensated transmission line using support vector machine. *IEEE Transactions on Power Delivery, 22(1),* 67–73. DOI 10.1109/tpwrd.2006.876695.
13. Jiang, J. A., Chen, C. S., Liu, C. W. (2003). A new protection scheme for fault detection, direction discrimination, classification, and location in transmission lines. *IEEE Transactions on Power Delivery, 18(1),* 34–42. DOI 10.1109/tpwrd.2002.803726.
14. Mahanty, R. N., Gupta, P. B. D. (2004). Aimlication of RBF neural network to fault classification and location in transmission lines. *IEE Proceedings-Generation Transmission and Distribution, 151(2),* 201–212. DOI 10.1049/ip-gtd:20040098.
15. Mirzaei, M., Kadir, M., Hizam, H., Moazami, E. (2011). Comparative analysis of probabilistic neural network, radial basis function, and feed-forward neural network for fault classification in power distribution systems. *Electric Power Components and Systems, 39(16),* 1858–1871. DOI 10.1080/15325008.2011.615802.
16. Parikh, U. B., Das, B., Maheshwari, R. (2010). Fault classification technique for series compensated transmission line using support vector machine. *International Journal of Electrical Power and Energy Systems, 32(6),* 629–636. DOI 10.1016/j.ijepes.2009.11.020.
17. Fahim, S. R., Sarker, Y., Sarker, S. K., Sheikh, M. R. I., Das, S. K. (2020). Self attention convolutional neural network with time series imaging based feature extraction for transmission line fault detection and classification. *Electric Power Systems Research, 187,* 12. DOI 10.1016/j.epsr.2020.106437.
18. Ye, W., Jian, S., Ou, R., Huang, S., Yuan, H. (2020). Fault classification of high voltage transmission line based on convolutional neural network. *2020 10th International Conference on Information Science and Technology (ICIST)*, pp. 294–300. DOI 10.1109/ICIST49303.2020.9201950.
19. Fuada, S., Shiddieqy, H. A., Adiono, T. (2020). A High-accuracy of transmission line faults (TLFS) classification based on convolutional neural network. *INTL Journal of Electronics and Telecommunications, 66(4),* 655–664. DOI 10.24425/ijet.2020.134024.
20. Galvao, R. K. H., Araujo, M. C. U., Jose, G. E., Pontes, M. J. C., Silva, E. C. et al. (2005). A method for calibration and validation subset partitioning. *Talanta, 67(4),* 736–740. DOI 10.1016/j.talanta.2005.03.025.
21. Zhang, R., Wang, L., Chen, D. (2021). An intelligent diagnosis method of the working conditions in sucker-rod pump wells based on convolutional neural networks and transfer learning. *Energy Engineering, 118(4),* 1069–1082. DOI 10.32604/EE.2021.014961.

22. Chen, W. X., Li, Y. N., Li, C. (2020). A visual detection method for foreign objects in power lines based on mask R-CNN. *International Journal of Ambient Computing and Intelligence, 11(1),* 34–47. DOI 10.4018/ijaci.2020010102.
23. He, F. S., He, Y., Liu, Z. G., Xu, C. A. (2020). Research and development on applications of convolutional neural networks of radar automatic target recognition. *Journal of Electronics and Information Technology, 42(1),* 119–131. DOI 10.11999/jeit180899.
24. Ni, H., Wang, M., Zhao, L. (2021). An improved faster R-CNN for defect recognition of key components of transmission line. *Mathematical Biosciences and Engineering, 18(4),* 4679–4695. DOI 10.3934/mbe.2021237.
25. Hu, Y. B., Zhang, J., Ma, Y., An, J. B., Ren, G. B. et al. (2019). Hyperspectral coastal wetland classification based on a multiobject convolutional neural network model and decision fusion. *IEEE Geoscience and Remote Sensing Letters, 16(7),* 1110–1114. DOI 10.1109/lgrs.2018.2890421.
26. Wang, Y. H., Li, Q. Q., Chen, B. (2019). Image classification towards transmission line fault detection via learning deep quality-aware fine-grained categorization. *Journal of Visual Communication and Image Representation, 64,* 6. DOI 10.1016/j.jvcir.2019.102647.